Environmental Science & Technology

Article

pubs.acs.org/est

Long-Term Evolution of Anthropogenic Heat Fluxes into a Subsurface Urban Heat Island

Kathrin Menberg,*[,†] Philipp Blum,[†] Axel Schaffitel,[†] and Peter Bayer[‡]

[†]Karlsruhe Institute of Technology (KIT), Institute for Applied Geosciences (AGW), Kaiserstrasse 12, 76131 Karlsruhe, Germany

[‡]ETH Zurich, Geological Institute, Sonneggstrasse 5, 8092 Zurich, Switzerland

Supporting Information

ABSTRACT: Anthropogenic alterations in urban areas influence the thermal environment causing elevated atmospheric and subsurface temperatures. The subsurface urban heat island effect is observed in several cities. Often shallow urban aquifers exist with thermal anomalies that spread laterally and vertically, resulting in the long-term accumulation of heat. In this study, we develop an analytical heat flux model to investigate possible drivers such as increased ground surface temperatures (GSTs) at artificial surfaces and heat losses from basements of buildings, sewage systems, subsurface district heating networks, and reinjection of thermal wastewater. By modeling the anthropogenic heat flux into the subsurface of the city of Karlsruhe, Germany, in 1977 and 2011, we evaluate long-term trends in the heat flux processes. It revealed that elevated GST and heat loss from basements are dominant factors in the heat anomalies. The average total urban heat flux into the shallow aquifer in Karlsruhe was found to be ~759 ± 89 mW/m^2 in 1977 and 828 ± 143 mW/m^2 in 2011, which represents an annual energy gain of around 1.0 × 10^{15} J. However, the amount of thermal energy originating from the individual heat flux processes has changed significantly over the past three decades.

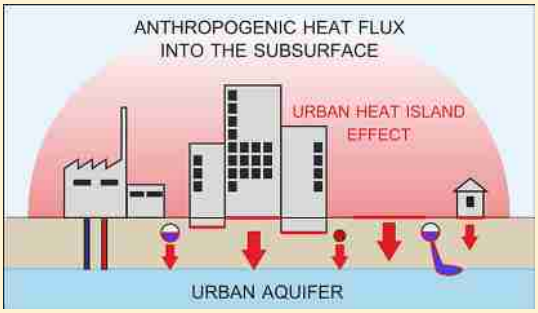

INTRODUCTION

Increasing temperatures due to anthropogenic alteration in urban areas are not solely found in the atmospheric environment [urban heat island effect (UHI)].[1−6] Also in the subsurface, human activities lead to significant and extensive warming, which causes urban aquifer temperatures to increase by several degrees.[7−11] Oke[12] gives a review of the studies that investigated the diverse processes and factors that lead to atmospheric UHI formation by examination of the urban energy balance. These efforts resulted in the development of various schemes for the quantification of urban heat fluxes into the atmosphere (i.e., upward) such as anthropogenic heat flux[13,14] and into the subsurface (i.e., downward) such as soil and ground heat flux.[15,16] The latter is thereby usually incorporated in the urban heat storage term and often calculated as the residual from the radiation balance at the surface.[16,17] Others developed analytical and numerical solutions to calculate the ground heat flux based on temperature or surface heat flux measurements.[18−20] Average measured and simulated values for monthly ground heat fluxes in urban areas were found to vary between −10 and 20 W/m^2, depending on the location and month of examination.[18,20] However, because of the complexity and heterogeneity of the urban environment, studies of ground heat flux yield only data with either spatially (e.g., remote sensed data)[17] or temporally high resolution (e.g., time series at single measurement points).[21] Another limitation of the commonly used atmospheric models concerning ground heat flux is their lower boundary condition. As discussed, for example, by Baker and Baker[22] and Kollet et al.,[23] the assumption of an adiabatic or fixed temperature boundary in the shallow subsurface (<10 m) seems unrealistic and can lead to substantial biases in long-term simulation of subsurface temperature and ground heat flux. Stevens et al.[24] showed that especially subsurface heat storage can be underestimated by up to 75%, if the bottom boundary condition is placed insufficiently deep, leading to significant errors in future climate projections.[25]

The changes in subsurface temperatures due to variations in ground surface temperature (GST) are also used for past climate reconstructions.[26,27] A common approach is to obtain GST histories and the corresponding ground surface heat flux histories by mathematical inversion of deep borehole temperatures.[28,29] Beltrami et al.[30] derived spatial patterns of heat gain in the subsurface of the Northern Hemisphere with a mean surface heat flux of ~21 mW/m^2 over the past 200 years based on 588 boreholes. Other studies scrutinized the coupling of surface air temperatures (SATs), GSTs, and shallow subsurface temperatures showing that the temperature offset is mainly influenced by surface cover and climate conditions.[31−33] However, studies of the evolution of urban subsurface temperature and GST are rare.[34] Taniguchi et al.[8] found

Received: April 10, 2013
Revised: July 27, 2013
Accepted: July 29, 2013
Published: July 29, 2013

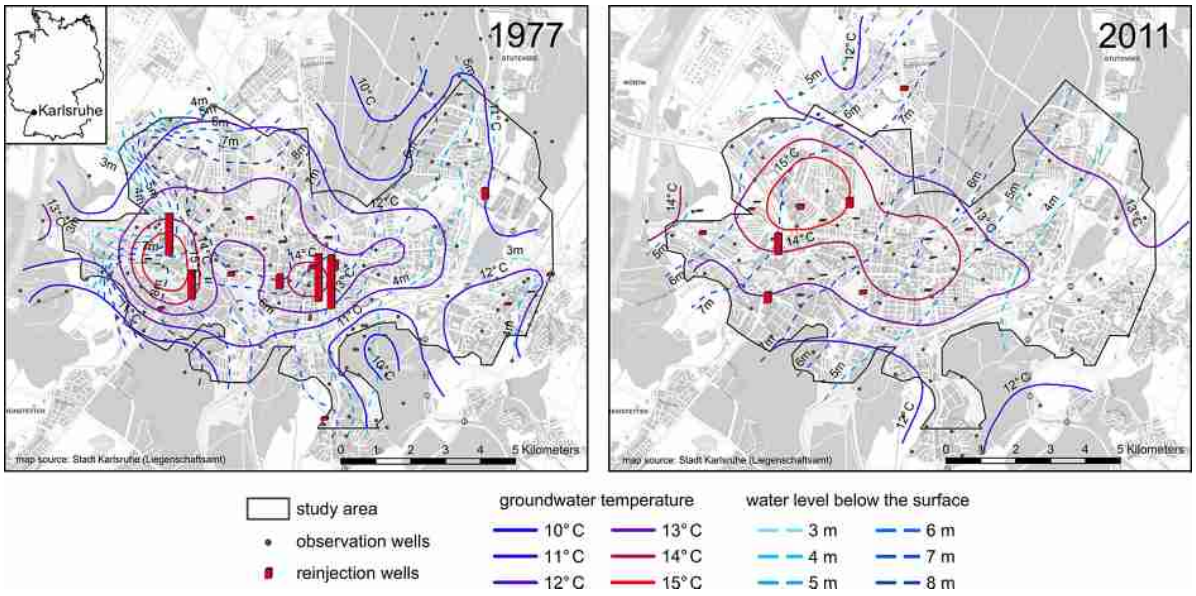

Figure 1. Location of the study area with contours of groundwater level and temperature. The groundwater temperature in 1977 was measured at the water surface and in 2011 3–4 m below the water level. The length of the bars indicates the reinjected energy amount per year. The bar in the legend represents ~0.5 MW. Note that both background images display a map of Karlsruhe in 2010.

temperature anomalies in the subsurface of four Asian megacities at depths of up to 140 m that correspond to the historic air temperature increase due to urbanization. Especially in built-up areas, solar irradiation of artificial surfaces leads to heterogeneously increased GST and thus ground heat fluxes.[35] Taylor and Stefan[36] investigated GSTs of different surface types in Minneapolis-St. Paul and found differences of up to 3 K in the annual mean GST between grass and asphalt cover.

The upper boundary of the urban subsurface is formed by not only open ground covered by different surface materials but also basements of buildings. The heat loss from basements or ground floors of single buildings into the ground has been examined for design and thermal comfort purposes.[37,38] Various analytical and numerical methods for predicting the seasonal heat loss for individual buildings with specific geometries and different kinds of insulation exist.[39,40] The applicability of such models to study processes on the urban scale, however, is limited.

In addition to the heat input from above, there are embedded anthropogenic heat sources that emit heat directly in the urban subsurface, like sewage networks, incompletely insulated district heating pipes, or reinjections of thermal wastewater.[11] However, until now, the question of which heat sources contribute what amounts to subsurface urban warming is unresolved. As pointed out by Taylor and Stefan[36] and Ferguson and Woodbury,[41] increased GST and heat loss from basements, respectively, cannot cause such extensive and widespread temperature anomalies like those found under most urban areas.

In this study, we focus on the heat input into shallow urban aquifers caused by various anthropogenic heat sources, which we define as the anthropogenic heat flux into the subsurface (AHF_s). The objective of this study is therefore to quantify the contribution of the individual heat processes that cause underground urban warming. A novel approach using an analytical heat flux model is developed for the city of Karlsruhe, Germany. To account for the uncertainty of the various input parameters and to identify the most relevant processes and parameters, we perform a Monte Carlo simulation and sensitivity analysis. Using a data set from 1977 and recent measurements from 2011, the long-term evolution of the subsurface urban heat island in Karlsruhe is comprehensively assessed by analyzing all dominant heat flux processes. The heat fluxes from buildings are spatially resolved for both years to also investigate the spatial temperature development.

MATERIALS AND METHODS

Study Area. As a study site, we chose the city of Karlsruhe because the subsurface temperature distribution was intensively investigated in the past and recently.[11,42,43] The study area is shown in Figure 1. It is delimited to the built-up area of Karlsruhe, covering urban, suburban, and industrial compartments, as well as inner city green spaces. The city is located in the upper Rhine Valley in southwest Germany, at approximately 49°00′ N and 8°24′ E, at a mean altitude of 115 m above sea level. The total population amounted to 275828 inhabitants in 1977 and increased to 294761 in 2011. The shallow subsurface geology in the study area is mainly composed of sand and gravel with minor contents of silt and clay.[44] The uppermost aquifer is unconfined and reaches a thickness of up to 30 m. The water level below the surface varies between 3 and 8 m, and the general groundwater flow direction is northwest to the Rhine River (Figure 1). Water level and shallow vertical groundwater temperature (GWT) profiles in 1977 were measured monthly at 142 observation wells by Makurat.[42] For 2011, we use daily values of water level and GWT from data loggers installed in 83 wells, which are operated by the Public Works Service Karlsruhe. Although only 41 of the original wells in 1977 could be used for measurements in 2011, both measurement campaigns yield representative regional GWT distributions because of the homogeneous distribution of the wells within the study area (Figure 1). Because of the fixed position of the data loggers in 2011, GWT in 2011 is only available at a depth of 3–4 m below the water table. The difference in GWT at the groundwater surface and 4 m below the surface in the 142 profiles in 1977 was found to be

Table 1. Assumed Parameter Ranges and Distributions for the Monte Carlo Simulations in 1977 and 2011

heat flux process	parameter	name	unit	year	minimum	mode	maximum	distribution
increased GSTs	λ	thermal conductivity (unsaturated zone)[a]	W m^{-1} K^{-1}		0.3	1	1.8	triangular
	dT	temperature difference of GST − GWT[b]	K	1977	0	1	5	triangular
				2011	0.8	1.8	5.8	triangular
	dz	depth of water table	m					spatial distribution
	A	study area	km^2		–	61.94	–	constant value
	A_b	area covered by buildings[c]	km^2	1977	10.34	10.88	11.43	triangular
				2011	12.37	13.02	13.67	triangular
buildings	T_b	temperature of basement/ground floor[d]	°C		15	17.5	20	triangular
	T_{gw}	groundwater temperature	°C					spatial distribution
	db	depth of basements	m					spatial distribution
reinjection of thermal wastewater	c_{pw}	heat capacity of water[e]	J kg^{-1} K^{-1}		–	4195	–	constant value
	γ_w	water density[e]	kg/m^3		–	999.8	–	constant value
	V_{ri}	volume of reinjected thermal wastewater[f]	m^3/a	1977	6408034	7209038	8010042	triangular
				2011	3526640	3967470	4408300	triangular
	T_{ri}	reinjection temperature[f]	°C	1977	20.4	22.7	24.9	triangular
				2011	18	20	22	triangular
sewage network	T_s	sewage temperature[g]	°C		12	18.5	25	triangular
	d_{sd}	diameter of sewage drains[h]	m		0.1	0.4	2	triangular
	ds	depth of sewage drains[i]	m		1	2	5	triangular
	l_{sn}	length of sewage network[j]	m	1977	532000	600000	665000	triangular
				2011	770000	880000	990000	triangular
	r_{dhf}	percentage of downward-directed heat flux	%		25	37.5	50	triangular
	r_{satm}	percentage of heat flux to atmosphere	%		20	30	40	triangular
sewage leakage	c_{ps}	heat capacity of wastewater[k]	J kg^{-1} K^{-1}		3708	4120	4532	triangular
	γ_s	density of wastewater[k]	kg/m^3		990	1100	1210	triangular
	V_s	annual wastewater volume[g]	m^3/a	1977	41259600	45844000	50428400	triangular
				2011	33997000	35707500	37418000	triangular
	r_l	leakage rate[h]	–		0.05	0.15	0.25	triangular
	r_{latm}	percentage of heat flux to atmosphere	%		20	30	40	triangular
district heating network	P_{ld}	heat loss from district heating pipes[l]	MW	1977	8.99	9.99	10.99	triangular
				2011	7.99	9.13	10.27	triangular

[a]From refs 50 and 51. [b]From refs 31, 36, and 45. [c]Mode estimated from Google Earth, ±5%. [d]Range from DIN EN ISO 13370.[52] [e]From ref 53. [f]Ninety percent of the licensed data;[42] Public Works Service Karlsruhe, ±10%. [g]From ref 42 and Public Works Service Karlsruhe. [h]Data from refs 48 and 49. [i]From the municipal water supplier of Karlsruhe.[54] [j]From ref 42 and the municipal water supplier of Karlsruhe,[54] ±10%. [k]From ref 42, ±10%. [l]Data from ref 42 and the municipal energy supplier of Karlsruhe, ±10%.

on average −0.1 ± 0.3 K, which is in the same range as the accuracy of the measurement device in 1977.[42] Thus, in 2011, the variability of GWT over this depth is expected to be minor and the temperatures from 3 to 4 m below the water table are adopted to approximate the GWT at the groundwater surface. The spatial distribution of the annual mean of the groundwater level and the GWT is shown in Figure 1 for 1977 and 2011. Also depicted are the locations of all reinjection wells, where cooling water (i.e., warm water injection) from, for example, industrial processes is discharged into the aquifer, and the total discharged energy.

In 1977, the highest GWT occurred in industrial areas close to major reinjection sites and in the city center. Compared to those in 1977, background temperatures in 2011 have increased by approximately 1 K, while the maximal GWT is nearly equal at ∼15 °C. However, the area of the thermal anomaly has spread significantly over the past three decades. In some areas, for example, in the northeastern parts, where a large residential area was developed, the GWT increased by even up to 2 K. The long-term development of major climate and groundwater parameters over the past decades in Karlsruhe is shown in Figure S1 of the Supporting Information. The mean annual SAT at a weather station outside of Karlsruhe was 10.7 °C in 1977 and increased to 11.5 °C in 2011, which is in agreement with the general long-term trend of SAT[45] (Figure S1a of the Supporting Information). This climatic trend is reflected in an increase in GWT in the rural background. The annual precipitation shows a slightly decreasing trend over the past decades (Figure S1b of the Supporting Information). In contrast, the water level indicates an opposite development of higher water tables. Here, reductions in the size of groundwater

dx.doi.org/10.1021/es401546u | Environ. Sci. Technol. 2013, 47, 9747−9755

withdrawals and the influence of the regional flow system are also important factors.

Heat Flux Model. To evaluate AHF_s, we developed a statistical analytical heat flux model. In this model, vertical heat fluxes from several heat sources through the unsaturated zone to the top of the groundwater body are considered. On the basis of spatial inspection of groundwater temperatures in several cities,[11] six individual heat flux processes q_i (eqs 2−6) are summed up in annual AHF_s analysis (eq 1).

$$AHF_s = \sum_{i=1}^{6} q_i \tag{1}$$

All model parameter values are listed in Table 1 and illustrated in Figure S2 of the Supporting Information.

The ground heat flux in our model is expressed as a heat flux process because of the increased GST and calculated by Fourier's law of heat conduction (eq 2).[46] We choose the temperature gradient in the unsaturated zone between the ground surface and the water table and apply the heat flux to that part of the study area that is not covered by buildings. The corresponding temperature difference is defined by the local variance between GST and GWT at the groundwater surface.

$$q_1 = \lambda \times dT/dz \times (A - A_b)/A \tag{2}$$

The heat flux from basements of buildings (eq 3) is also calculated based on Fourier's law and applied to the area covered by buildings. Here, only the heat flux through the basement floor is considered. The heat flux through the basement walls is neglected, because experimental and modeling studies of the heat loss through basements showed that the heat loss through the walls is mainly connected to the atmosphere.[37,38] Likewise, the increased heat flux that can be observed at the edges of a basement is primarily upward directed. Thus, we assume no correction factor for edge effects or building geometries. The temperature gradient is set between the air temperature inside the basement and the GWT. The thermal conductivity in eq 3 is the integral conductivity of the basement slab and the soil underneath.

$$q_2 = \lambda \times (T_b - T_{gw})/(dz - db) \times A_b/A \tag{3}$$

As Fourier's law describes only conduction, advective heat transport, for example, by infiltration, is neglected. Infiltration of surface water in urban areas is assumed to be low because of the high rate of surface sealing.[47] Thus, vertical advective heat transport in the study area is expected to be rather small. The heat input due to reinjections of thermal wastewater is assessed by the energy content of the amount of water and the temperature difference between withdrawal and reinjection:

$$q_3 = c_{pw}\gamma_w V_{ri} \times (T_{ri} - T_{gw})/A \tag{4}$$

Two heat flux processes are thought to arise from the sewage system. The first is a conductive heat flow from the pipes of the sewage network, which are partly filled with wastewater of a certain temperature and emit heat to some extent upward as well as downward:

$$q_4 = \lambda \times (T_s - T_{gw})/(dz - ds) \times (d_{sd}\pi l_{sn})/A \times r_{dhf} \times (1 - r_{satm}) \tag{5}$$

Additionally, sewage leakage occurs to some degree from all sewage pipes.[48,49] The energy content of the leaked water is calculated and assumed to partly reach the water table:

$$q_5 = c_{ps}\gamma_s V_s r_l \times (T_s - T_{gw})/A \times (1 - r_{latm}) \tag{6}$$

As the city of Karlsruhe operates a widespread district heating network, also heat losses from the underground district heating pipes are considered to cause a partly downward directed heat flux:

$$q_6 = P_{ld} \times r_{dhf}/A \tag{7}$$

The methods for the calculation of heat fluxes q_3 and q_6 were adopted from ref 42. The author estimated average heat fluxes in the shallow subsurface mostly based on literature values such as solar irradiation and heat loss from buildings. As a consequence, that approach yields partly unreasonable results when it is applied for the entire city.

Monte Carlo Simulation. Most of the parameters of the heat flux equations in Table 1 cannot be captured with single values for the entire study area; thus, parameter ranges are specified. Some parameters, such as groundwater temperature or thermal conductivity of the unsaturated zone, show strong spatial and temporal variability. For other parameters, such as leakage rate or sewage temperature, measured data are not available for the study area, so that the chosen representative literature values carry uncertainty. To consider the entire range of possible input parameters, the heat flux is calculated with a Monte Carlo approach with a defined statistical distribution for each parameter. Few parameters can be assessed with a fixed value, such as the size of the study area. For the other parameters, a triangular distribution was assumed by defining minimal and maximal values, as well as a mode value with the highest probability.

The difference in local GST and GWT, dT, is thought to range between 0 and 5 K. In long-term steady-state examinations, mean annual GST and shallow GWT are usually assumed to equal each other (e.g., ref 36), with no heat flux occurring into the subsurface. Alteration of the surface cover leads to a change in GST. Changes from vegetated surfaces to bare soil were found to cause an increase in annual mean GST between 0.3 and 1 K, while concrete and asphalt surfaces show a GST that is 2−5 K higher than at a grass or forest site.[31,36] The percentages of different surface types in the study area were estimated on the basis of a land use plan, similar to the approach of Taylor and Stefan.[36] According to the land use plan of Karlsruhe, ∼20% of the study area is covered by buildings and the rest is characterized by different kinds of vegetation (∼56%) and artificial surface covers (∼24%). Because of this distribution and the fact that the GWT below the urban area is already elevated compared to the undisturbed background, the mode value for dT is set to 1 K. As the annual mean SAT in 2011 was 0.8 K higher than in 1977,[45] this value was added to the triangular distribution, given that GST usually track SAT in long-term trends.[33] For the depth of the water table, the groundwater temperature, and the depth of basements, we derived spatially resolved values from an interpolated raster data set in GIS (ESRI ArcInfo 10.0) (Figure 1). Thus, the heat flux from buildings can be calculated for each raster pixel by assigning probabilistic values for the parameters that are not spatially known. The number of Monte Carlo iterations is adapted to the number of raster pixels and set to 275257 runs. A detailed description of the assumed values for the other

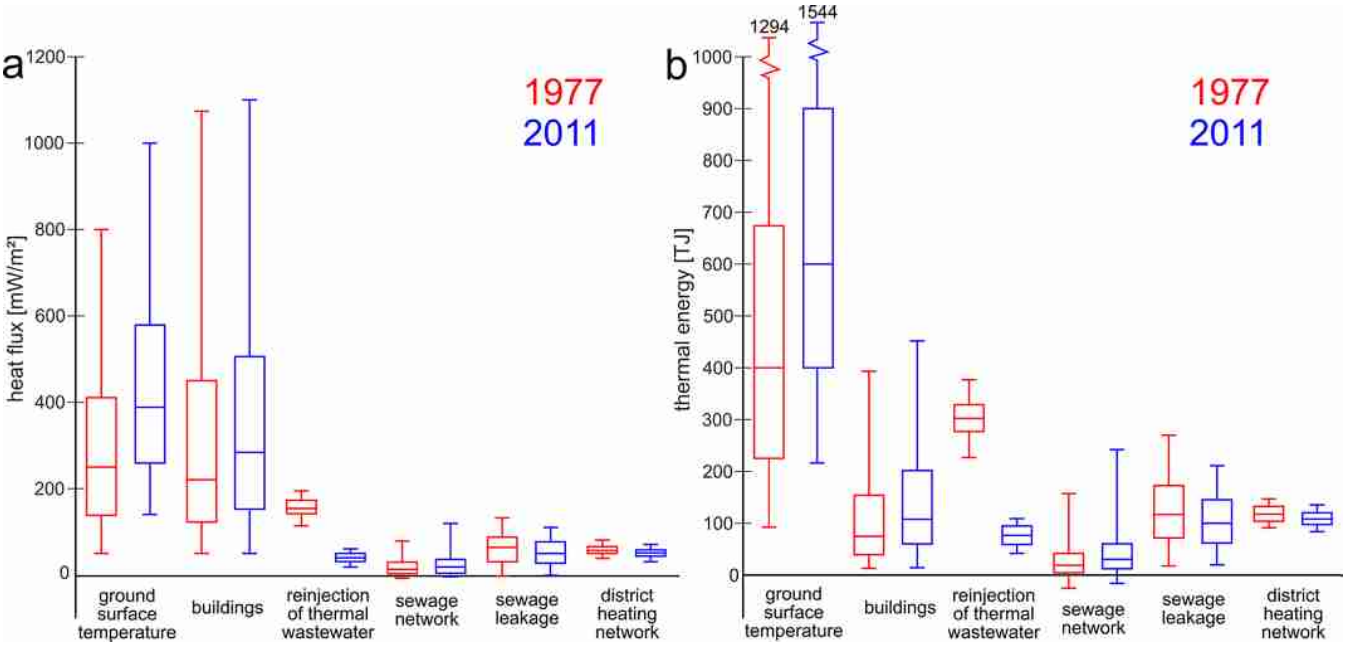

Figure 2. Results of the Monte Carlo simulation for 1977 and 2011. (a) Boxplots of the individual heat fluxes. (b) Thermal energy amounts per year for the entire study area caused by the individual heat flux processes (lower end of 5% and upper end of 95% of the entire range).

parameter ranges is given in the Supporting Information. Finally, a contribution to variance analysis is performed by calculating Spearman's rank correlation coefficients between the total heat flux result and the individual input parameters.

RESULTS AND DISCUSSION

Monte Carlo Simulation. The total sum of the median heat fluxes and standard deviations from all considered heat sources was 759 ± 89 mW/m^2 in 1977 and 828 ± 143 mW/m^2 in 2011. The results of the Monte Carlo simulation for the individual heat fluxes are displayed in Figure 2a. The highest heat fluxes occur from the increased GST (249 ± 245 mW/m^2 in 1977 and 391 ± 277 mW/m^2 in 2011) and from buildings (224 ± 440 mW/m^2 in 1977 and 276 ± 481 mW/m^2 in 2011). The rather large standard deviations resemble the large ranges covered by the boxplots in Figure 2a. They are caused by the wide ranges assessed for the parameters in the heat flux equations (Table 1; for details, see the Supporting Information), which account for the high spatial and temporal variability over the study area. The other simulated processes are of minor relevance, contributing <10% to the total AHF_s. The negative heat fluxes from the sewage network can occur when the sewage temperature is lower than the groundwater temperature. Likewise, leakages in sewers can also cause the infiltration of groundwater into the sewers in places where the pipes are installed below the water table.

In comparison to these determined urban heat fluxes, the natural heat fluxes in the subsurface yield much smaller values. The geothermal heat flux in the area of Karlsruhe is ~80 mW/m^2.[55] A spatial analysis of the ground heat flux in rural areas caused by climate warming yielded values of 25−75 mW/m^2 for the period of 1930−1980 in Middle Europe.[30] These natural background heat fluxes are ~10 times lower than the total AHF_s; thus, the subsurface heat balance in the urban area in Karlsruhe is obviously dominated by anthropogenic heat sources.

According to the study of Flanner,[14] the atmospheric AHF due to anthropogenic energy use is between 2.5 and 4.0 W/m^2 in southwest Germany, which is ~4 times higher than the AHF_s calculated in this study. However, the atmospheric AHF value is integrated regionally and contains also rural areas with less anthropogenic heat emission. Thus, the atmospheric AHF for urban areas alone is likely to be even higher.

Figure 2b shows the amount of thermal energy that is discharged into the subsurface by the individual heat flux processes. From this evaluation, it becomes obvious that most of the ground heat gain is caused by increased GST (39% in 1977 and 59% in 2011). Because of a small area of coverage by buildings in Karlsruhe, the influence from buildings is generally weak (7% in 1977 and 11% in 2011), despite the high heat flux density. The spatial distribution of the heat flux from buildings is subsequently discussed. Thermal energy input from reinjections of thermal wastewater (29% in 1977 and 8% in 2011), sewage leakage (12% in 1977 and 10% in 2011), and the district heating network (11% in 1977 and 10% in 2011) is comparable to the heat input from buildings. However, these processes are constrained to distinct positions, such as reinjection wells or failures in sewage and district heating pipes. Thus, they cause only very local thermal anomalies in the groundwater. Such local heat sources could explain the heterogeneous GWT distribution that is often observed beneath cities.[8,11] In contrast, an increased GST and buildings influence the subsurface on a larger area and can therefore cause extensive thermal anomalies.

The mean amount of energy discharge accounts for up to 1.0 × 10^{15} ± 1.4 × 10^{14} J for 1977 and remains almost equal for 2011 (1.0 × 10^{15} ± 1.9 × 10^{14} J). However, the amount of thermal energy arising from the individual heat flux processes mostly changed over the past three decades. The mean heat input from the elevated GST increased by 50% from 4.0 × 10^{14} to 6.0 × 10^{14} J in 2011. This represents a trend that is likely to continue with future temperature development due to climate change.[56]

dx.doi.org/10.1021/es401546u | Environ. Sci. Technol. 2013, 47, 9747−9755

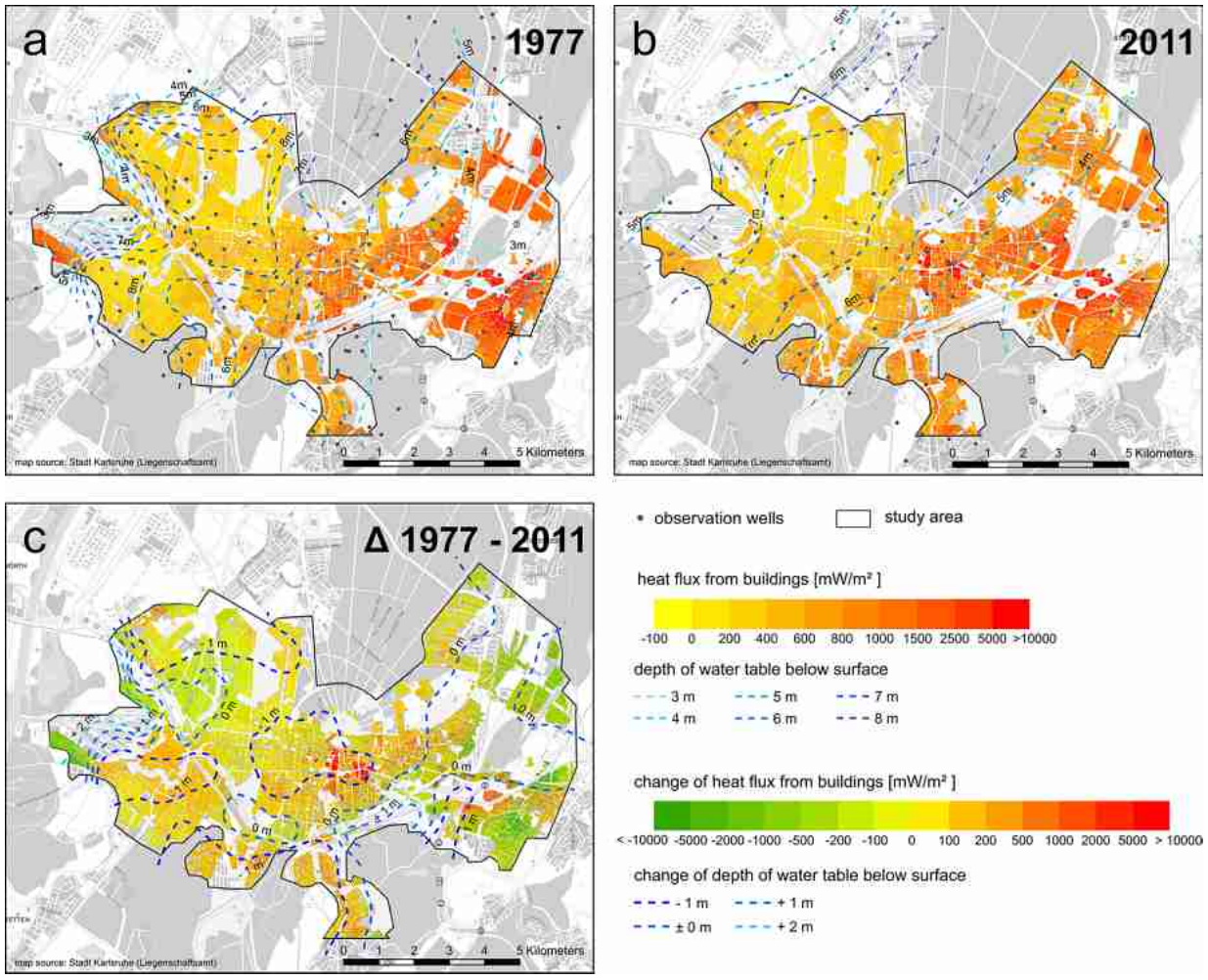

Figure 3. Spatial heat flux from buildings in 1977 (a) and 2011 (b). Panel c shows the changes in the spatial heat flux from buildings and the change in the depth of the water table from 1977 to 2011.

The heat flux from reinjections of thermal wastewater was relatively high in 1977 but decreased in 2011 because of legal regulations on allowed reinjection temperature and also because of a reduction in the reinjection volume. Variations in the other heat fluxes are mostly due to changes in specific parameter values (i.e., properties). Heat flux from the sewage network has increased because of the longer sewage network in 2011 that reflects the development of new residential districts in the study area. Despite the longer sewage network, the reduction in wastewater volume leads to a decrease in heat loss by sewage leakage. The trend of decreasing wastewater volume is a prevalent phenomenon in German cities caused by water saving measures. The district heating network in Karlsruhe was likewise expanded to new residential areas; even so, the heat loss from the network was reduced by maintenance and insulation actions.

Spatial Heat Flux from Buildings. The heat flux from buildings in Karlsruhe exhibits a considerable spatial heterogeneity (Figure 3a,b) with a large range between −100 and >10000 mW/m^2. Via comparison of spatial heat flux and the contours of water table depth, it becomes obvious that the vertical distance is the dominating factor for the computed temperature gradient.

Furthermore, buildings with deep basements, such as shopping malls and underground parking lots in the city center, caused local hot spots in 2011. This strong dependence of the heat loss from buildings on the existence of shallow groundwater has been previously observed in other studies.[41,57] The high heat fluxes in the southeastern part of Karlsruhe were also promoted by the relatively low GWT (Figure 1) that resulted in a high temperature gradient. Although this area is a rather old city district, the GWT in 1977 and in 2011 was low, because it was significantly influenced by an inflow of thermally unaffected groundwater from the rural background, which was estimated to be ∼520 m^3/day. Because of the chosen statistical approach, such advective effects were not adequately considered. However, the range of heat flux values obtained is in good agreement with the heat loss under individual basements in other studies, which reached 2−28 W/m^2 depending on the site parameters, such as depth of the water table and the thermal conductivity of the soil.[37,39,41,58] These studies, as well as our model, do not regard thermal insulation of basements. In Germany, ground slab insulation was not considered in construction regulations until the late 1990s.[59] Thus, most buildings in the study area are expected to have no insulation.

Compared to suburban areas (in particular in the eastern part of the city), the inner and western city revealed low to moderate heat fluxes, which were caused by not only a deep water table but also a higher GWT (Figure 1). At some

dx.doi.org/10.1021/es401546u | Environ. Sci. Technol. 2013, 47, 9747−9755

locations in the western part of the city, even negative heat fluxes occurred, which indicated an annual heat input from the ground into the basements, because basement temperatures were probabilistically assigned and therefore could be lower than the annual GWT. Figure 3c displays the changes in the heat flux from buildings and the spatial changes of the water table from 1977 to 2011, which were mainly caused by modifications of groundwater pumping (Figure 1). Green areas indicating a decrease in heat flux from buildings are mainly situated in the western parts, where the water level has decreased by up to 2 m, and in the eastern districts, where the groundwater temperature has increased (Figure 1). Rising heat fluxes could be observed in areas with an elevated water table that were surrounded by the −1 m isolines, e.g., in the southwestern part and in some areas in the eastern part. The most significant rise of the heat flux was located in the city center (red pixels), where several deep underground parking garages and basements have been constructed over the past decades. The superposition of these effects of variable depths of the water table, groundwater temperature, basement depth, and building density leads to a spatially heterogeneous development of heat flux from buildings.

Contribution to Variance Analysis. The highest Spearman's rank correlation coefficients for the model parameters are shown in Figure 4. The other parameters revealed correlation

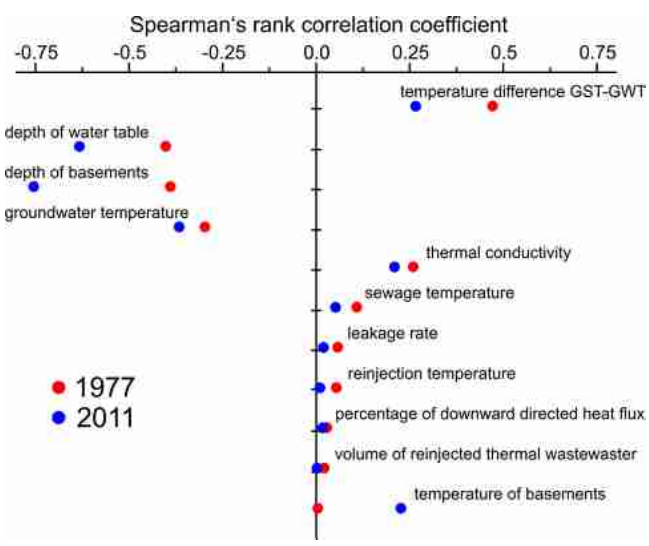

Figure 4. Results of the contribution to variance analysis displayed as Spearman's rank correlation coefficients between the heat flux result and the individual parameters. Only parameters with a correlation coefficient of >0.02 are shown here. The results for all parameters and the 95% confidence intervals are listed in Table S1 of the Supporting Information.

coefficients of <0.02 (Table S1 of the Supporting Information) and have, therefore, an only weak influence on the model outcome. The significance of the individual correlations was tested by calculating the 95% confidence interval that revealed rather close ranges (Table S1 of the Supporting Information). Parameters contributing to the large heat flux from the increased GST and buildings exhibited the highest sensitivities. The changes in the correlation coefficients between 1977 and 2011 are the result of the superposition of several effects. They are linked to not only changes in the parameter ranges but also changes in the relative contribution of the individual heat fluxes to the AHF_s (Figure 2a).

It can be stated that the important parameters either are known from spatial measurements, such as the depth of the water table and groundwater temperature, or can be assumed within a reasonable range, such as the thermal conductivity of the subsurface. The annual GST difference represents another major influencing factor. This effect of GST variations on subsurface temperatures in urban areas has also been examined by Ferguson and Woodbury,[9] who observed a correlation between the GWT and different land use types, which exhibits a varying GST. Also, changes in land surface cover, such as deforestation or surface sealing, were found to cause strong perturbations of the GST and consequently of subsurface temperatures.[36,60,61] Smerdon et al.[62] showed that climatic factors such as snow cover influence the land surface processes and the propagation of temperature signals into the subsurface. Thus, the temporal and spatial distribution of the GST in urban areas is expected to be rather heterogeneous. However, measured values of the spatial distribution of GST in urban areas are rare, although they could reduce the uncertainty of heat flux estimation (Figure 2) and consequently improve spatial heat flux analysis.

Although the values obtained with the model in this study apply only for the city of Karlsruhe, the discussed heat flux processes occur in many urban areas.[11] Most cities have a high building density and a high percentage of artificial surface covers. Consequently, the heat fluxes from the increased GST and buildings are expected to be the driving forces for subsurface warming in many urban areas. The heat input by the other minor heat sources depends mainly on the local circumstances, such as reinjections of thermal wastewater or district heating networks and on the length and condition of the sewage system. These factors substantially vary in each city, but the assumed parameter ranges in this study are rather large. Thus, it seems unlikely that the relative contribution of the individual components of the AHF_s will change significantly for other cities. Hence, urban areas are prone to exhibit extensive temperature anomalies in shallow aquifers with GWTs increased by several degrees.[11] Such significant temperature changes influence the chemical and biological properties of groundwater and also affect water quality.[63,64] Although most chemical processes are not expected to change significantly below 30 °C,[65] redox reactions are especially influenced by small temperature variations.[66,67] Water temperature also affects the diversity of aquifer bacteria and fauna[68,69] that play an important role in water purification and filtration.[64] On the other hand, an elevated GWT in urban areas also enhances the geothermal potential[10] and microbiological activity in the groundwater, which can promote biological remediation of organic contaminations in such urban or industrial areas.[70]

■ ASSOCIATED CONTENT

Supporting Information

Figures S1 and S2, Table S1, and a detailed description of the assumed parameter ranges for the Monte Carlo simulation. This material is available free of charge via the Internet at http://pubs.acs.org.

■ AUTHOR INFORMATION

Corresponding Author

*Phone: +49-721-6084-5011. Fax: +49-721-606-279. E-mail: kathrin.menberg@kit.edu.

Notes

The authors declare no competing financial interest.

■ ACKNOWLEDGMENTS

The financial support of K.M. via the Scholarship Program of the German Federal Environmental Foundation (DBU) is gratefully acknowledged. Furthermore, we thank Susanne Reimer, Friedhelm Fischer, and Ralf Schneider (Public Works Service Karlsruhe), Annette März (Environmental Service, City of Karlsruhe), and Manuel Rink (Stadtwerke Karlsruhe GmbH) for their valuable support with data and additional information. Special thanks go to Valentin Wagner for his support with MATLAB.

■ ABBREVIATIONS

AHF	anthropogenic heat flux
AHF_s	anthropogenic heat flux into the subsurface
GST	ground surface temperature
GWT	groundwater temperature
SAT	surface air temperature
SUHI	subsurface urban heat island
UHI	urban heat island

■ REFERENCES

(1) Oke, T. R. City size and the urban heat island. *Atmos. Environ.* **1973**, *7* (8), 769−779.
(2) Landsberg, H. E. *The Urban Climate*; Academic Press: New York, 1981.
(3) Arnfield, J. A. Two decades of urban climate research: A review of turbulence, exchanges of energy and water, and the urban heat island. *Int. J. Climatol.* **2003**, *23*, 1−26.
(4) Schwarz, N.; Lautenbach, S.; Seppelt, R. Exploring indicators for quantifying surface urban heat islands of European cities with MODIS land surface temperatures. *Remote Sensing of Environment* **2011**, *115* (12), 3175−3186.
(5) Peng, S.; Piao, S.; Ciais, P.; Friedlingstein, P.; Ottle, C.; Bréon, F.; Nan, H.; Zhou, L.; Myneni, R. Surface urban heat island across 419 global big cities. *Environ. Sci. Technol.* **2012**, *46*, 696−703.
(6) Schwarz, N. Comment on "Surface Urban Heat Island Across 419 Global Big Cities". *Environ. Sci. Technol.* **2012**, *46* (12), 6888.
(7) Changnon, S. A. A rare long record of deep soil temperatures defines temporal temperature changes and an urban heat island. *Clim. Change* **1999**, *42* (3), 531−538.
(8) Taniguchi, M.; Uemura, T.; Jago-on, K. Combined Effects of Urbanization and Global Warming on Subsurface Temperature in Four Asian Cities. *Vadose Zone J.* **2007**, *6* (3), 591−596.
(9) Ferguson, G.; Woodbury, A. D. Urban heat island in the subsurface. *Geophys. Res. Lett.* **2007**, *34* (23), L23713.
(10) Zhu, K.; Blum, P.; Ferguson, G.; Balke, K.-D.; Bayer, P. The geothermal potential of urban heat islands. *Environ. Res. Lett.* **2010**, *5* (4), 044002.
(11) Menberg, K.; Bayer, P.; Zosseder, K.; Rumohr, S.; Blum, P. Subsurface urban heat islands in German cities. *Sci. Total Environ.* **2013**, *442*, 123−133.
(12) Oke, T. R. The urban energy balance. *Progress in Physical Geography* **1988**, *12* (4), 471−508.
(13) Ichinose, T.; Shimodozono, K.; Hanaki, K. Impact of anthropogenic heat on urban climate in Tokyo. *Atmos. Environ.* **1999**, *33*, 3897−3909.
(14) Flanner, M. G. Integrating anthropogenic heat flux with global climate models. *Geophys. Res. Lett.* **2009**, *36* (2), L02801.
(15) Mirzaei, P. A.; Haghighat, F. Approaches to study Urban Heat Island: Abilities and limitations. *Building and Environment* **2010**, *45* (10), 2192−2201.
(16) Roberts, S. M.; Oke, T. R.; Grimmond, C. S. B.; Voogt, J. A. Comparison of Four Methods to Estimate Urban Heat Storage. *Journal of Applied Meteorology and Climatology* **2006**, *45*, 1766−1781.
(17) Rigo, G.; Parlow, E. Modelling the ground heat flux of an urban area using remote sensing data. *Theor. Appl. Climatol.* **2007**, *90*, 185−199.
(18) Wang, J.; Bras, R. L. Ground heat flux estimated from surface soil temperature. *J. Hydrol.* **1999**, *216*, 214−226.
(19) Bennett, W. B.; Wang, J.; Bras, R. L. Estimation of Global Ground Heat Flux. *Journal of Hydrometeorology* **2008**, *9*, 744−759.
(20) Wang, Z.-H.; Bou-Zeid, E. A novel approach for the estimation of soil ground heat flux. *Agricultural and Forest Meteorology* **2012**, *154*−*155*, 214−221.
(21) Herb, W. R.; Janke, B.; Mohseni, O.; Stefan, H. G. Ground surface temperature simulation for different land covers. *J. Hydrol.* **2008**, *356*, 327−343.
(22) Baker, J. M.; Baker, D. G. Long-term ground heat flux and heat storage at a mid-latitude site. *Clim. Change* **2002**, *54*, 295−303.
(23) Kollet, S. J.; Cvijanovic, I.; Schüttemeyer, D.; Maxwell, R. M.; Moene, A. F.; Bayer, P. The Influence of Rain Sensible Heat and Subsurface Energy Transport on the Energy Balance at the Land Surface. *Vadose Zone J.* **2009**, *8*, 846−857.
(24) Stevens, M. B.; Smerdon, J. E.; Gonzalez-Rouco, J. F.; Stieglitz, M.; Beltrami, H. Effects of bottom boundary placement on subsurface heat storage: Implications for climate model simulations. *Geophys. Res. Lett.* **2007**, *34* (2), L02702.
(25) MacDougall, A. H.; González-Rouco, J. F.; Stevens, M. B.; Beltrami, H. Quantification of subsurface heat storage in a GCM simulation. *Geophys. Res. Lett.* **2008**, *35* (13), L13702.
(26) Bodri, L.; Cermak, V. Climate changes of the last millennium inferred from borehole temperatures: Results from the Czech Republic Part I. *Global and Planetary Change* **1995**, *11*, 111−125.
(27) Pollack, H.; Huang, S.; Shen, P. Climate Change Record in Subsurface Temperatures: A Global Perspective. *Science* **1998**, *282*, 279−281.
(28) Huang, S.; Pollack, H.; Shen, P. Temperature trends over the past five centuries reconstructed from borehole temperatures. *Nature* **2000**, *403*, 756−758.
(29) Beltrami, H. Climate from borehole data: Energy fluxes and temperatures since 1500. *Geophys. Res. Lett.* **2002**, *29* (23), 26.
(30) Beltrami, H.; Bourlon, E.; Kellman, L.; Gonzales-Rouco, J. F. Spatial patterns of ground heat gain in the Northern Hemisphere. *Geophys. Res. Lett.* **2006**, *33* (6), L06717.
(31) Dědeček, P.; Šafanda, J.; Rajver, D. Detection and quantification of local anthropogenic and regional climatic transient signals in temperature logs from Czechia and Slovenia. *Clim. Change* **2012**, *113* (3−4), 787−801.
(32) Smerdon, J. E.; Pollack, H.; Enz, J. W.; Lewis, M. J. Conduction-dominated heat transport of the annual temperature signal in soil. *J. Geophys. Res.* **2003**, *108* (B9), 2431.
(33) Smerdon, J. E.; Pollack, H.; Cermak, V.; Enz, J. W.; Kresl, M.; Safanda, J.; Wehmiller, J. F. Air-ground temperature coupling and subsurface propagation of annual temperature signals. *J. Geophys. Res.* **2004**, *109* (21), D21107.
(34) Yamano, M.; Goto, S.; Miyakoshi, A.; Hamamoto, H.; Lubis, R. F.; Monyrath, V.; Taniguchi, M. Reconstruction of the thermal environment evolution in urban areas from underground temperature distribution. *Sci. Total Environ.* **2009**, *407*, 3120−3128.
(35) Kottmeier, C.; Biegert, C.; Corsmeier, U. Effects of Urban Land Use on Surface Temperature in Berlin: Case Study. *Journal of Urban Planning and Development* **2007**, *133* (2), 128−137.
(36) Taylor, C. A.; Stefan, H. G. Shallow groundwater temperature response to climate change and urbanization. *J. Hydrol.* **2009**, *375*, 601−612.
(37) Thomas, H. R.; Rees, S. W. The thermal performance of ground floor slabs: A full scale in-situ experiment. *Building and Environment* **1999**, *34*, 139−164.

(38) Emery, A. F.; Heerwagen, D. R.; Kippenhan, C. J.; Steele, D. E. Measured and Predicted Thermal Performance of a Residential Basement. *HVAC&R Res.* **2007**, *13* (1), 39−57.
(39) Adjali, M. H.; Davies, M.; Littler, J. G. Earth-contact heat flows: Review and application of design guidance predictions. *Building Services Engineering Research and Technology* **1998**, *19* (3), 111−121.
(40) Rees, S. W.; Adjali, M. H.; Zhou, Z.; Davies, M.; Thomas, H. R. Ground heat transfer effects on the thermal performance of earth-contact structures. *Renewable Sustainable Energy Rev.* **2000**, *4* (3), 213−265.
(41) Ferguson, G.; Woodbury, A. D. Subsurface heat flow in an urban environment. *J. Geophys. Res.* **2004**, *109* (2), B02402.
(42) Makurat, A. Analyse der Temperaturschwankungen des Grundwassers im Stadtgebiet von Karlsruhe. Diploma Thesis, Universität Karlsruhe (TH), Karlsruhe, Germany, 1980.
(43) Hötzl, H.; Makurat, A. Veränderungen der Grundwassertemperaturen unter dicht bebauten Flächen am Beispiel der Stadt Karlsruhe. *ZDGG* **1981**, *132*, 767−777.
(44) Geyer, O. F.; Gwinner, M. P. *Geologie von Baden-Württemberg*; Schweizerbart: Stuttgart, Germany, 2011.
(45) Deutscher Wetterdienst: Web-based Weather Request and Distribution System (http://www.dwd.de/) (accessed March 20, 2013).
(46) Weber, S. Comparison of in-situ measured ground heat fluxes within a heteorogeneous urban ballast layer. *Theor. Appl. Climatol.* **2006**, *83*, 169−179.
(47) Liu, C.; Shi, B.; Tang, C.; Gao, L. A numerical and field investigation of underground temperatures under Urban Heat Island. *Building and Environment* **2011**, *46* (5), 1205−1210.
(48) Eiswirth, M.; Held, I.; Hötzl, H.; Wolf, L. Abwasser im urbanen Grundwasserleiter: Stoffeintrag, Umsetzungen und Gefährdungspotential. In Progress Report, Forschergruppe Kanalleckage: Gefährdungspotential von Abwasser aus undichten Kanälen für Boden und Grundwasser; Universität Karlsruhe: Karlsruhe, Germany, 2002.
(49) Klinger, J. Beschreibung der Wasser- und Stoffflüsse in einem urbanem Raum unter besonderer Berücksichtigung von Kanalleckagen. Ph.D. Dissertation, Universität Karlsruhe (TH), Karlsruhe, Germany, 2007.
(50) Menberg, K.; Steger, H.; Zorn, R.; Reuss, M.; Proell, M.; Bayer, P.; Blum, P. Bestimmung der Wärmeleitfähigkeit im Untergrund durch Labor- und Feldversuche und anhand theoretischer Modelle (Determination of thermal conductivity in the subsurface using laboratory and field experiments and theoretical models). *Grundwasser* **2013**, *18* (2), 103−116.
(51) Verein Deutscher Ingenieure. VDI 4640-1: Thermische Nutzung des Untergrundes—Grundlagen, Genehmigungen, Umweltaspekte (Thermal use of the underground—Fundamentals, approvals, environmental aspects); Beuth Verlag GmbH: Berlin, 2010.
(52) Deutsches Institut für Normung e.V. DIN EN ISO 13370: Wärmetechnisches Verhalten von Gebäude—Wärmeübertragung über das Erdreich (Thermal performance of buildings—Heat transfer via the ground); Beuth Verlag GmbH: Berlin, 2008.
(53) Clauser, C. *Geothermal Energy*; Springer-Verlag: Berlin, 2006.
(54) Stadt Karlsruhe. Tiefbauamt Karlsruhe: Die Stadtentwässerung in Karlsruhe (http://www.karlsruhe.de/b3/bauen/tiefbau/entwaesserung/entwaesserungsgebuehr/HF_sections/content/ZZk9uVuzOo24XJ/ZZk9uWfqOuhpKP/Tiefbauamt_Broschuere_2010.pdf) (accessed March 20, 2013).
(55) Cermak, V.; Rybach, L. *Terrestrial heat flow in Europe*; Springer-Verlag: Berlin, 1979.
(56) IPCC Fourth Assessment Report (AR4). Climate Change 2007: Synthesis Report, Contribution of Working Groups I, II and III to the Fourth Assessment Report of the Intergovernmental Panel on Climate Change; Geneva, 2007.
(57) Rees, S. W. The influence of soil moisture content variations on heat losses from earth-contact structures: An initial assessment. *Building and Environment* **2001**, *36*, 157−165.
(58) Kusuda, T.; Bean, J. W. Simplified Methods for Determining Seasonal Heat Loss from Uninsulated Slab-on-Grade Floors. *ASHRAE Trans.* **1984**, *84* (11), 611−632.
(59) Deutsches Institut für Normung e.V. DIN 4108-2: Wärmeschutz und Energie-Einsparung in Gebäuden—Teil 2: Mindestanforderungen an den Wärmeschutz (Thermal protection and energy economy in buildings—Part 2: Minimum requirements to thermal insulation); Beuth Verlag GmbH: Berlin, 2011.
(60) Nitoiu, D.; Beltrami, H. Subsurface effects of land use changes. *J. Geophys. Res.* **2005**, *110*, F01005.
(61) Taniguchi, M.; Shimada, J.; Tanaka, T.; Kayane, I.; Sakura, Y.; Shimano, Y.; Dapaah-Siakwan, S.; Kawashima, S. Disturbances of temperature-depth profiles due to surface climate change and subsurface water flow: 1. An effect of linear increase in surface temperature caused by global warming and urbanization in the Tokyo metropolitan area, Japan. *Water Resour. Res.* **1999**, *35* (5), 1507−1517.
(62) Smerdon, J. E.; Beltrami, H.; Creelman, C.; Stevens, M. B. Characterizing land surface processes: A quantitative analysis using air-ground thermal orbits. *J. Geophys. Res.* **2009**, *114*, D15102.
(63) Green, T. R.; Taniguchi, M.; Kooi, H.; Gurdak, J. J.; Allen, D. M.; Hiscock, K. M.; Treidel, H.; Aureli, A. Beneath the surface of global change: Impacts of climate change on groundwater. *J. Hydrol.* **2011**, *405*, 532−560.
(64) Hähnlein, S.; Bayer, P.; Ferguson, G.; Blum, P. Sustainability and policy for the thermal use of shallow geothermal energy. *Energy Policy* **2013**, *59*, 914−925.
(65) Bonte, M.; Stuyfzand, P. J.; Hulsmann, A.; van Beelen, P. Underground thermal energy storage: Environmental risks and policy developments in the Netherlands and European Union. *Ecology and Society* **2011**, *16* (1), 22.
(66) Prommer, H.; Stuyfzand, P. J. Identification of Temperature-Dependent Water Quality Changes during a Deep Well Injection Experiment in a Pyritic Aquifer. *Environ. Sci. Technol.* **2005**, *39* (7), 2200−2209.
(67) Jesußek, A.; Grandel, S.; Dahmke, A. Impacts of subsurface heat storage on aquifer hydrogeochemistry. *Environ. Earth Sci.* **2013**, *69* (6), 1999−2012.
(68) Hall, E. K.; Neuhauser, C.; Cotner, J. B. Toward a mechanistic understanding of how natural bacterial communities respond to changes in temperature in aquatic ecosystems. *ISME J.* **2008**, *2* (5), 471−481.
(69) Brielmann, H.; Griebler, C.; Schmidt, S. I.; Michel, R.; Lueders, T. Effects of thermal energy discharge on shallow groundwater ecosystems. *FEMS Microbiol. Ecol.* **2009**, *68* (3), 242−254.
(70) Slenders, H. L. A.; Dols, P.; Verburg, R.; Vries, A. J. d. Sustainable remediation panel: Sustainable synergies for the subsurface: Combining groundwater energy with remediation. *Remediation* **2010**, *20*, 143−153.